



PROCEEDINGS OF SPIE
SPIE—The International Society for Optical Engineering

Optical Wireless Communications V

Eric J. Korevaar
Chair/Editor

1 August 2002
Boston, Massachusetts, USA

Sponsored and Published by
SPIE—The International Society for Optical Engineering



Volume 4873

SPIE is an international technical society dedicated to advancing engineering and scientific applications of optical, photonic, imaging, electronic, and optoelectronic technologies.



The papers appearing in this book comprise the proceedings of the meeting mentioned on the cover and title page. They reflect the authors' opinions and are published as presented and without change, in the interests of timely dissemination. Their inclusion in this publication does not necessarily constitute endorsement by the editors or by SPIE.

Please use the following format to cite material from this book:

Author(s), "Title of paper," in *Optical Wireless Communications V*, Eric J. Korevaar, Editor, Proceedings of SPIE Vol. 4873, page numbers (2002).

ISSN 0277-786X
ISBN 0-8194-4652-1

Published by
SPIE—The International Society for Optical Engineering
P.O. Box 10, Bellingham, Washington 98227-0010 USA
Telephone 1 360/676-3290 (Pacific Time) · Fax 1 360/647-1445

Copyright © 2002, The Society of Photo-Optical Instrumentation Engineers.

Copying of material in this book for internal or personal use, or for the internal or personal use of specific clients, beyond the fair use provisions granted by the U.S. Copyright Law is authorized by SPIE subject to payment of copying fees. The Transactional Reporting Service base fee for this volume is \$15.00 per article (or portion thereof), which should be paid directly to the Copyright Clearance Center (CCC), 222 Rosewood Drive, Danvers, MA 01923. Payment may also be made electronically through CCC Online at <http://www.directory.net/copyright/>. Other copying for republication, resale, advertising or promotion, or any form of systematic or multiple reproduction of any material in this book is prohibited except with permission in writing from the publisher. The CCC fee code is 0277-786X/02/\$15.00.

Printed in the United States of America.

Conference Committee

Conference Chair

Eric J. Korevaar, Optical Access, Inc. (USA)

Program Committee

Pierre R. Barbier, TeraBeam Networks (USA)

David L. Begley, Ball Aerospace & Technologies Corporation (USA)

Theresa H. Carbonneau, fSONA Communications Corporation (Canada)

James E. Freidell, Daedalian Technologies Ltd. (USA)

G. Stephen Mecherle, fSONA Communications Corporation (USA)

Paul F. Szajowski, TeraBeam Networks (USA)

Contents

v Conference Committee

SESSION 1 OUTDOOR FREE-SPACE OPTICS I

- 1 **Simulating atmospheric free-space optical propagation: II. Haze, fog, and low clouds attenuations** [4873-01]
M. Achour, UlmTech, Inc. (USA)

SESSION 2 INDOOR OPTICAL WIRELESS SYSTEMS I

- 13 **Integrated CMOS transmitter driver and diversity receiver for indoor optical wireless links** [4873-02]
D. M. Holburn, V. A. Lalithambika, R. J. Samsudin, V. M. Joyner, R. J. Mears, Univ. of Cambridge (United Kingdom); J. Bellon, M. J. N. Sibley, Univ. of Huddersfield (United Kingdom)
- 23 **Flip-chip integrated optical wireless transceivers** [4873-03]
D. C. O'Brien, G. E. Faulkner, E. B. Zyambo, D. J. Edwards, Univ. of Oxford (United Kingdom); P. N. Stavrinou, G. Parry, Imperial College (United Kingdom); J. Bellon, M. J. N. Sibley, Univ. of Huddersfield (United Kingdom); V. A. Lalithambika, V. M. Joyner, R. J. Samsudin, D. M. Holburn, R. J. Mears, Univ. of Cambridge (United Kingdom)
- 30 **Eye-safe collimated laser emitter for optical wireless communications** [4873-04]
P. Benítez, J. C. Miñano, F. J. López, D. Biosca, R. Mohedano, M. Labrador, F. Muñoz, Univ. Politécnica de Madrid (Spain); K. Hirohashi, M. Sakai, HITS Labs., Inc. (Japan)
- 41 **Power-efficient multiple-subcarrier modulation scheme for optical wireless communications** [4873-05]
B. Yu, Univ. of California/Berkeley (USA) and Stanford Univ. (USA); J. M. Kahn, R. You, Univ. of California/Berkeley (USA)
- 54 **Biorthogonal DSSS for infrared wireless communications on non-Lambert reflection channels** [4873-06]
H. T. Zhang, M. L. Gong, P. Yan, K. Zhang, S. S. Zou, X. Yang, W. Jin, F. Jiang, Tsinghua Univ. (China)
- 63 **Indoor infrared wireless communication system based on Ethernet network** [4873-07]
X. Yang, M. L. Gong, K. Zhang, H. T. Zhang, P. Yan, W. Jin, F. Jiang, Y. Meng, S. S. Zou, Tsinghua Univ. (China)
- 71 **Simulation of impulse response on IR wireless indoor channel with concentrator** [4873-08]
X. Yang, M. L. Gong, H. T. Zhang, P. Yan, S. S. Zou, W. Jin, K. Zhang, F. Jiang, Y. Meng, Tsinghua Univ. (China)

SESSION 3 OUTDOOR FREE-SPACE OPTICS II

- 79 **Comparison between experimental and theoretical probability of fade for free-space optical communications** [4873-09]
A. Al-habash, K. W. Fischer, C. S. Cornish, K. N. Desmet, J. Nash, Terabeam Corp. (USA)
- 90 **Stress-Optic beam stabilization in free-space optics** [4873-10]
G. A. Seaver, SeaLite Engineering, Inc. (USA)

SESSION 4 OUTDOOR FREE-SPACE OPTICS III

- 99 **Background light environment for free-space optical terrestrial communications links** [4873-11]
D. Rollins, J. Baars, D. P. Bajorins, C. S. Cornish, K. W. Fischer, T. Wiltsey, Terabeam Corp. (USA)
- 111 **Product testing of free-space optical transceivers** [4873-12]
R. Stieger, E. G. Kaetz, Terabeam Corp. (USA)
- 121 **Acquisition in short-range free-space optical communication** [4873-13]
J. Wang, J. M. Kahn, Univ. of California/Berkeley (USA)
- 133 **Solar background effects in wireless optical communications** [4873-14]
V. G. Sidorovich, Sunflower Technologies Ltd. (USA)
- 143 **Hybrid FSO radio (HFR): some preliminary results** [4873-18]
S. H. Bloom, W. S. Hartley, AirFiber (USA)
- 155 **Debunking the recurring myth of a magic wavelength for free-space optics** [4873-19]
E. J. Korevaar, I. I. Kim, B. McArthur, MRV Communications (USA)
- 167 *Addendum*
- 168 *Author Index*

Simulating Atmospheric Free-Space Optical Propagation, Part II: Haze, Fog and Low Clouds Attenuations

Maha Achour, Ph.D.*

UlmTech, Inc. 4215 Camino Sandoval, San Diego, CA 92130

Abstract

One of the biggest challenges facing Free-Space Optics deployment is proper understanding of optical signal propagation in different atmospheric conditions. In an earlier study by the author [30], attenuation by rain was analyzed and successfully modeled for infrared signal transmission. In this paper, we focus on attenuation due to scattering by haze, fog and low clouds droplets using the original Mie Scattering theory. Relying on published experimental results on infrared propagation, electromagnetic waves scattering by spherical droplets, atmospheric physics and thermodynamics, UlmTech developed a computer-based platform, Simulight™, which simulates infrared signal (750 nm-12 μ m) propagation in haze, fog, low clouds, rain and clear weather. Optical signals are scattered by fog droplets during transmission in the forward direction preventing the receiver from detecting the minimum required power. Weather databases describe foggy conditions by measuring the visibility parameter, which is, in general, defined as the maximum distance that the visible 550 nm signal can travel while distinguishing between the target object and its background at 2% contrast. Extrapolating optical signal attenuations beyond 550 nm using only visibility is not as straightforward as stated by the Kruse equation which is unfortunately widely used. We conclude that it is essential to understand atmospheric droplet sizes and their distributions based on measured attenuations to effectively estimate infrared attenuation. We focus on three types of popular fogs: Evolving, Stable and Selective.

Keywords: Free-space optics, optical wireless, atmospheric modeling, infrared propagation, Mie scattering, rainfall attenuation, non-selective scattering, Rayleigh scattering, Visibility, fog, haze, low clouds.

1. Introduction

Since early 2001, the Telecom industry has experienced a setback in broadband communication networks deployments. Few of the factors contributing to the continuing telecom downturn are the collapse of the data communication business model, the uncontrolled telecom deregulation act of 1986, lack of the broadband killer application and the formidable investments that poured into the industry and led to fierce and unfair competition. On the service providers' side, business operation couldn't be sustained without end-users' subscription and commitment to their service offerings. According to a February report issued by the U.S. Federal Communications Commission (FCC), only 7%, or 7.5 million of U.S. households with broadband access are subscribed to high-speed Internet access services as of June 2001. Of course lack of broadband applications is one of the major reasons for this low percentage. In fact, many households are still using phone lines for their Internet access because of the. Synchronous online learning is emerging as the leading killer broadband application bringing a new concept of learning, anytime, anywhere, from variety of choices and on a global scale. A key factor to successfully provide such services is to maintain an acceptable Quality of Service (QoS) during the learning session. In general, most of the added-value-services that are under consideration by service providers, to augment their failing data service offering, require adequate QoS. In fact, these added-value-services can be implemented overnight due to network protocol and Operational Support System (OSS) maturity.

Another factor preventing end-users addition to the broadband network is the missing last link, or first link if viewed from users prospective, to the network. This challenge is refereed to by the last mile problem. As wireless technologies bypass many last mile obstacles in term of right of way and cost of wiring the region, unlicensed

* Contact email: machour@ulmtech.com; Web: <http://www.ulmtech.com>; Phone: 858-336 6965; Fax: 858-794 9628

wireless is by far the most desirable solution due to its “instantaneous” deployment feature. One of the main concerns of wireless technologies is their communication link availability when QoS is required by service providers.

In the past few years, Free-Space Optics (FSO) has emerged as the wireless continuum of fiber for up to few kilometers range. FSO global license-free aspect distinguishes it from other unlicensed wireless technology in term of its Marketing potential. The biggest challenge facing FSO deployment, however, is its performance in different weather conditions such as fog. Simulight™, a software product developed by UlmTech, was released in March 2002 to bring a common factor analysis of FSO weather performance. Simulight™ is considered the first fully integrated and functional simulation tool that models wireless infrared signal propagation in the atmosphere. In reference [30], the author discussed the effect of rain on FSO propagation.

An alternative path for FSO, which seems to be getting more attention, is instead of focusing on FSO weather performance, service providers are considering backup links instead. In light of our analysis, such a direction is more practical because of the difficulties laying in estimating FSO link availability. Looking at the frequency spectrum, 60 GHz, and hopefully soon higher frequencies up to 120 GHz, microwave products are under consideration as potential backup links to FSO or simply main communications links. Simulight™ is in the process of integrating these high frequencies into its weather performance side by side with FSO.

In this paper we model the propagation of infrared signals in few fog, haze and low clouds cases using the original Mie scattering equation along with droplets size distribution. Since Simulight™ technology relies on its unique distribution derivation; we will review the thermodynamics and mechanics of these weather condition formations and refrain from providing the mechanism used to derive the corresponding droplet distribution. Simulight™ spans wavelengths between 750 nm to 12 μ m which were considered using published references and experimental results. Mie scattering due to aerosol and fog droplet distribution, which is by far the most complex to simulate, is considered the major atmospheric element that attenuates the optical signal.

Modeling FSO atmospheric propagation requires different types of input information. We classify these inputs in three categories:

Deployment parameters: These are parameters related to the location and application of the FSO system installation such as Range, Bandwidth, and Wavelength.

FSO system parameters: These are parameters related to the deployed FSO system: number of transmitters (Tx) and Receivers (Rx), Tx diameter, Rx diameter, Tx power, Rx sensitivity, additional amplification, and additional hardware losses.

Weather parameters: For example, meteorological visual Range (visibility), temperature, relative humidity (or dewpoint), fog model (non-selective, evolving, and stable).

This paper is organized as follows; in section two we review the physics behind fog and low cloud formation, in section 3 we review the main weather parameters utilized through FSO attenuation derivation process, in section 4 we present some Simulight™ distribution models and compare them to some experimental results and finally we state our conclusion in section 5.

2. Atmospheric Physics

The atmosphere is this gaseous envelope surrounding the Earth. Due to the gravitational force, which contributes to atmospheric pressure, the maximum density occurs just above the surface of the Earth and gradually becomes thinner as we move away from the surface. In this paper, we focus on the layer near the surface where FSO systems are deployed for terrestrial communication. At these altitudes, the atmosphere essentially acts as a fluid in hydrostatic equilibrium. Thermodynamics refers to the study of conservation, properties of matter, and energy conversion including the relationship between energy and the changes. The classical and quantum mechanical principals governing thermodynamics are known as statistical mechanics. For purposes of understanding fog and cloud formations and evolutions, only classical mechanics is hence considered [1]. Most of this section's discussion is derived from reference [28].

Water vapor concentration is highest near Earth surface; an indication that Earth surface is the principal source of atmospheric water vapor. Thermodynamically, water is the only substance in the atmosphere that occurs naturally in all three phases of matter with condensed water consisting of suspended water droplet particles (fog, cloud) and hydrometeors (raindrops, snow). In addition, the atmosphere composition includes uncondensated aerosol particles: dust, sea-salt particles, soil particles, volcano debris, pollen, by-products of combustion and other small particles that arise from chemical reactions with the atmosphere [28]. In general, Aerosol particles sizes ranges between 0.1 and 10 μ with drop-size concentration dropping sharply with increasing drop sizes. Density refers to the mass of the atmosphere per unit volume. A typical value of surface air is around 1.3 Kg/m³. The *mean free path* of atmospheric particles, which is determined by the frequency of inter-particle collisions [19,28], is inversely proportional to density. The *mean free path* increases exponentially from about 0.1 μ at surface to 1 m at 100 Km above the surface. Water contributes to the increase in air density due to the high density of water, $\rho_w = 10^3$ Kg/m³ at 4°C and 1 atm pressure. In the atmosphere we have a mixture of dry air and water vapor governed by the following effects and parameters:

- Partial pressure of water vapor e
- Partial pressure of dry air P_d
- Total atmospheric pressure $P = e + P_d$
- Water vapor saturation, which refers to the case when the air includes the maximum liquid water quantity that it can hold, pressure with respect to liquid water is e_s
- Relative Humidity is equal to

$$HR = \frac{e}{e_s} \quad (1)$$

In contrast to gases, which expand to fill the volume of their container, condensed phases can maintain a free boundary (surface) and occupy a definite volume. During droplets initial formations, the interface between the liquid and its vapor is not a two-dimensional surface, but rather a zone that is several molecules thick; over which the concentration of water varies continuously until the equilibrium state is reached. Water molecules at the surface of droplet are subject to external interaction as well as internal with neighboring molecules but cannot freely move inside the droplet. When the forces surrounding the surface molecules are asymmetric with inward net force, surface molecules will move towards the interior of the droplet until equilibrium is attained. This effect is due to droplet surface expansion because the energy of the surface molecule of the liquid becomes higher than the energy in the interior. Surface effect is due to the surface tension work, which is proportional to the surface area, and the energy necessary to extend the liquid surface against the vapor surrounding it. Therefore, the liquid surface is created as a result of an increase in the potential energy. Spherical shapes have the smallest surface area for a given volume, and hence the smallest surface energy. Hence, the spherical shape of cloud and fog drops results from the minimum-energy principle.

Nucleation of Water Droplets in the Atmosphere

A fraction of the collisions between water vapor molecules in the atmosphere are inelastic, *i.e.* merging molecules, leading to the formation of molecule aggregations which have a short lifetime since they disintegrate under continuous molecule bombardment. When the aggregated water droplet reaches a size sufficient for survival, the nucleation of water droplet then occurs. An embryo water droplet nucleation is a result of energy supplied by droplet's surrounding to form its surface. This form of energy comes in the form of latent heat of condensation. Since the surface tension is proportional to the area (πr^2) and latent heat is proportional to the drop mass, then a critical radius is attained when the surface tension work balances the latent heat. This critical radius r^* represents the threshold for nucleation.

Fog and cloud drops are formed by *heterogeneous* nucleation of some Aerosol particles that are *hygroscopic*, *i.e.* attract water vapor molecules to their surface through chemical processes or physical forces caused by the presence of hydrogen dipole. This effect may occur below 100% humidity. For example the deliquescent point of salt (NaCl) is about RH=75%. Another factor contributing to droplet growth is the collection model where small drops collide to form larger drops. One efficient model of such a phenomenon is called the scholastic collection model that accounts for the probabilistic aspects of collision and coalescence. Using the stochastic model, some drops are "statistically favored" for rapid growth as illustrated in figure (1). Let us consider the following example, if we start with 100 drops, all having the same radius. If we assume that 10% of the drops undergo collision in one second, after two seconds one statistically favored drop triples its mass while 81 of the drops remain at their initial size.

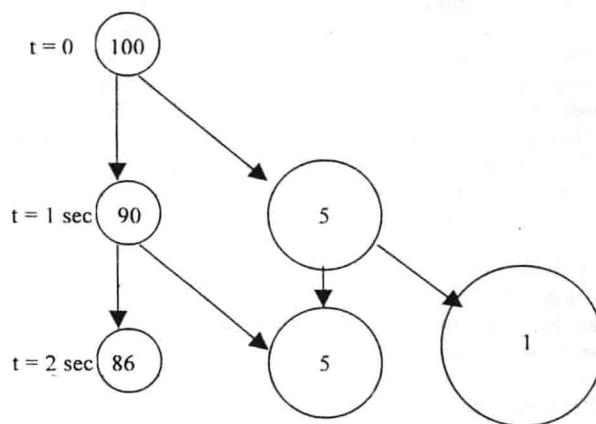


Fig. 1: Illustration of an example of stochastic collection model.

Cloud condensation nuclei (CCN) are considered a subset of *hygroscopic* aerosol particles where nucleation of pure water drops may occur at supersaturating less than 1%. For drops below the critical nucleation radius r^* , the drops grow only in response to increase in relative humidity and termed haze particles. A condensation nucleus is said to be activated when the drop formed on it grows to size r^* . Once the drop grows slightly beyond r^* , its equilibrium value of supersaturation is less than the supersaturation at the critical radius formation. As it will be explained later, droplet size distribution in the atmosphere will sometime exhibits two radius peaks instead of one. This is referred to as bimodal distributions. Stochastic collection along with the equilibrium of droplets with its surrounding contributes to the bimodal size distribution explanation.

The explanation of the observed broadening of drop size spectra $n(r)$ remains a major challenge to cloud and fog physicists. Fog is composed of very small water drops in suspension in the atmosphere, which greatly reduces visibility. It is mainly caused by cooling of air to its dew point and the addition of water vapor in the air. Fog may be considered as a stratus cloud whose base is low enough to reach the ground. Fog, stratus and stratocumulus clouds occur within 2 km from the ground. They are not associated with precipitation, although often produce drizzle.

Classification				Aitken	Large	Giant
Size Ranges for:	Air Electricity	Small ions	Large ions			
	Atm Optics				Haze	
	Cloud Phys.				Active CCN	
	Air Chemistry				Particles mainly contributing to Aerosol Mass	
Particle radius in μ		10^{-3}	10^{-2}	10^{-1}	10^0	10^1

Fig. 2: Classification of Aerosol particles [7].

Aerosols

The atmospheric aerosol forms a particle spectrum which spans over four orders of magnitude sizes, and are subdivided into four categories as described below and illustrated in figure 2 [7]:

- Aitken particles: The smallest particles less than or equal to 0.1 μ .
- Larger particles: Their corresponding sizes ranges between 0.1 and 1 μ .
- Giant particles: For radius greater than 1 μ .

It is important to emphasize that Aerosol terminology in the context of our studies includes nuclei resulting from water vapor condensation regardless of their physical or chemical properties. In figure 2, large particles are responsible for scattering visible and near infrared rays. Furthermore, only large and giant nuclei become activated as condensation nuclei because the required water vapor supersaturation is always small. Aitken nuclei, however, remain inactive with smooth line separating the active from the inactive nuclei [7] because of the higher supersaturation levels required to condensate Aitken particles. This is another phenomenon contributing to the bimodal water droplet distribution models. As relative humidity increases, Aerosol particles gradually grow to become cloud, fog or ice droplets.

In general, many methods of measuring particle size distribution are simultaneously needed to cover the whole spectrum of figure 2. Due to this complex measuring mechanism, frequently one method is used restricting the outcome to a subset of the whole spectrum [4,7,18]. For instance, particles below 0.1 μ are commonly derived from the diffusion parameter whereas particles between 0.1-0.5 μ may be collected using electrical or thermal precipitation. Particles larger than 0.5 μ are derived from a light scattering instrument. Furthermore, it has been noted that Aerosol size concentration is further classified between continental and maritime measurements as indicated in table 1 [7].

Table 1: Example of particle concentrations for continental and maritime regions [7].

Particle concentration of radius (μ)								
	< 0.01	0.01-0.032	0.032-0.1	0.1-0.32	0.32-1	1-3.2	> 3.2	Total number
Continental	1600	6800	5800	940	29	0.94	0.029	15,169
Maritime	3	83	105	14	2	0.47	0.029	207

The most important properties of an Aerosol mix are their size variations with relative humidity. Particle radius grows until equilibrium between the droplet and its surrounding is attained. For soluble particle, equilibrium depends on the initial particle size and its salt mass content. At equilibrium, the relative humidity of salt droplets indicates that the influence of the dissolved salt decreases more rapidly with increasing size than does the influence of surface curvature. Therefore, the growth curve passes the 100% humidity line, reaches a maximum and then approach the 100% humidity line asymptotically. In other word, water vapor condensation requires the particle to be in an unstable supersaturation state with its surrounding to continuously grow. For giant and large particles, the critical supersaturation amounts to only few tenths of a percent (for example 100.01%), whereas it increases rapidly to several percents (for example 100.1%) for Aitken particles. As mentioned earlier, this phenomenon also contributes to the bimodal size distribution explanation.

The supersaturation is of great importance for cloud and fog formation. When air is cooled and fog droplets start to form, only the largest condensation particle with lowest supersaturation start to grow. Smaller particles, however, often do not reach their peak because they require much higher supersaturation level and remain on the stable branch of the growth curve. We schematically illustrate this effect in figure 3 to explain the bimodal size distribution effect.

In most literature, the basic assumption in size distribution calculations was that the temperature and humidity fields are completely uniform throughout the fog or cloud. In reality, there are always fluctuations that are depicted in the gap between the inactivated and activated curves in figure 3. Due to aerosol combination of mixed nuclei and the non-linear dependence of supersaturation with the particle size, the dividing gap between the inactivated and activated particles is smoothed out giving birth to a second maximum, *i.e.* bimodal distribution size distribution function.

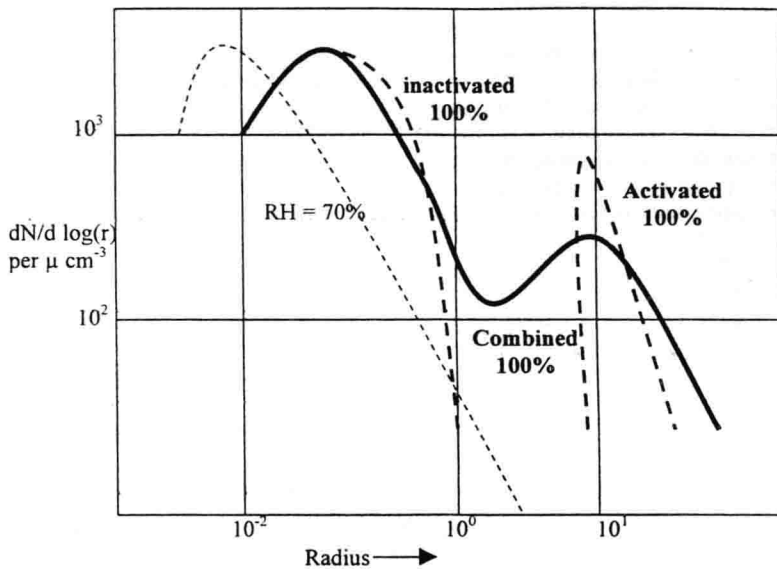


Fig. 3: Schematic diagram of activated and inactivated nuclei condensation of continental aerosol [1963 Junge].

Equivalent Water Content

Given an Aerosol-size distribution $n(r)$ defined by the equation below

$$n(r) = \frac{dN(r)}{dr} \quad (\text{cm}^{-3} \text{ per } \mu) \quad (2)$$

The total number of Aerosol particle is given by

$$N_{\text{Total}} = \int n(r) dr \quad (\text{cm}^{-3}) \quad (3)$$

The Equivalent Water Content (EWC) of such an Aerosol mixture is given by

$$\text{EWC}_{\text{Total}} = \rho_w \int \frac{4}{3} \pi r^3 n(r) dr \quad (\text{gr cm}^{-3}) \quad (4)$$

Where, ρ_w is the water density equal to $10^{-12} \text{ gr } \mu^{-3}$. Equation 4 includes soluble particles with the approximation of water density excluding the amount of diluted salt. Given the third power radius in equation (4) integrant, particles smaller than 3μ contribute very little to the equivalent water content and therefore could be neglected with respect to the presence of giant particles [7]. Most of references cover this important aspect of size distributions and liquid water equivalence [7,9].

3. Weather Parameters

In calculating attenuation due to haze, fog and low clouds, the weather parameters necessary are visibility, temperature and relative humidity.

Meteorological Visual Range

Meteorological visual range (Visibility) is the most important weather parameter needed to estimate FSO attenuation due to haze, fog and low clouds attenuation. Unlike other weather parameters, visibility measurements have improved throughout the years leading to more accurate numbers. The challenge still remains in how to relate the visibility measurements to atmospheric attenuation based on measurement techniques. Our first assumption is that visibility is measured using the lowest level of 2% contrast that the eye can detect. The general definition of relative contrast is as follows [2,17,20,29]:

$$\frac{C(V)}{C(0)} = \frac{L_{\max}(V) - L_{\min}(V)}{L_{\min}(V)} \frac{L_{\min}(0)}{L_{\max}(0) - L_{\min}(0)} \equiv \frac{L_{\max}(V)}{L_{\max}(0)} = e^{-\alpha V} \quad (5)$$

Where, L refers to the object (max) and background (min) luminance. In the above equation, two approximations were made. The first valid assumption is that background intensity is much inferior to the object intensity, *i.e.* $L_{\min}(0) \ll L_{\max}(0)$. The second assumption is that the horizon is considered as the background, *i.e.* $L_{\min}(0) = L_{\min}(V)$. With recent advents in color-based camera, more precise measurement of visibility can be conducted using more complex derivations of contrast. In summary, visibility is defined as the maximum distance at which the object contrast against its background is 2% using 550 nm wavelengths that the eye is most sensitive to. Considering the above two assumptions, visibility can be related to the extinction coefficient $\beta(\lambda=0.55\mu)$ by the following relation:

$$V = \frac{|\ln(0.02)|}{\beta(\lambda = 0.55\mu)} = \frac{3.91}{\beta(\lambda = 0.55\mu)} \text{ (Km)} \quad (6)$$

Once the visibility is obtained, extending this value to attenuations to longer wavelengths is not trivial and requires extensive modeling of the optical channel for different wavelengths.

Absolute humidity is defined as the mass of water vapor in a unit volume of air.

Saturation refers to the maximum possible amount of water vapor that air can hold per unit volume. It is temperature dependent.

Dew Point refers to the temperature at which saturation occurs.

Relative humidity is the ratio of the absolute humidity to saturation as defined in equation (1). This parameter, along with temperature, is useful to determine additional water absorption due to water vapor presence in the air.

4. Haze, Fog and Low Cloud Attenuation

The atmospheric attenuation τ_a is described by the following Beer's law equation:

$$\tau_a = e^{-(\beta_{\text{abs}} + \beta_{\text{scat}})R} \quad (7)$$

Where, β_{abs} and β_{scat} are the absorption and scattering coefficient, respectively. In some literature, τ_a is also referred to as the atmospheric transmittance or simply the transmittance of optical depth R . Fog droplet distribution, formation and evolution represent a challenging problem because it crosses many scientific areas: thermodynamics, cloud physics and boundary-layer meteorology [7,8,15,16,20]

Absorption:

Absorption by atmospheric gases defines the atmospheric windows [2,6,9,12,24,25,26], whereas millimeter waves' windows are defined by H_2O and O_2 absorption. There are many quantum-mechanical models that describe molecular absorption such as the popular Air Force Geophysics Laboratory AFGL codes FASCODE, MODTRAN and LOWTRAN [26]. Nitrogen and Oxygen are by far the most abundant atmospheric gases. Oxygen has a relatively narrow absorption bands around 60 GHz because of magnetic dipole moment, at 760 nm and has strong absorption in the ultraviolet band. Neither of these gases has any absorption bands in the infrared spectrum. However, they are important for Rayleigh scattering and refractive index computation.

Ironically, some the most important molecules impacting propagation, H_2O and CO_2 , have variable concentration. Water vapor is highly variable from day to day, season to season, with altitude, and for different geographical locations. Its air volume ratio varies between 0 and 2% [26]. Carbon dioxide varies seasonally with maximum concentration during the early spring and a minimum concentration during the late summer to early fall. Its concentration runs between 0.03 to 0.04 percent [25]. The variable nature of these atmospheric gases makes the prediction of atmospheric propagation at infrared frequencies a challenge.

Simulight™ provides users with an estimation of the absorption window and warn them when the selected wavelength falls between two atmospheric windows.

Atmospheric Scattering

It is interesting to note that most of the light that reaches our eyes comes indirectly by means of scattering. Fine particles or bits of matter standing in the path of continuous transmission of electromagnetic waves abstract energy from the incident wave and re-radiate it in different directions. Forward scattering becomes more significant when particles sizes exceed the incident wavelength. Scattering by light is classified into the following three types:

Rayleigh scattering refers to scattering by molecular and atmospheric gazes of sizes much less than the incident light wavelength. It varies as the fourth power of the incident wavelength with overall constant dependent on the index of refraction.

Mie scattering occurs when the particle diameter is larger than one-tenth of the incident wavelength. Mie theory is applicable for scattering by isotropic spherical elements without quantum consideration of particle radiation by incident monochromatic light.

Non-selective scattering applies for particle sized larger than the incident wavelength. In this case, Mie theory is approximated by the principles of reflection, refraction and diffraction. The name non-selective refers to the fact that scattering is independent of wavelength.

For the Aerosol distribution in equation (2), the total scattering coefficient is derived from the following equation [9,11,12,13,17,20,23,24]:

$$\beta_{scatt}(\lambda) = \sum_i \pi r^2 n_i Q_{scatt}(x) \quad (Km^{-1}), \text{ where } x = \frac{2 \pi r}{\lambda} \tag{8}$$

Where, Q_{scatt} is the scattering efficiency, also referred to by the Mie attenuation coefficient in some references. For ratios $a/\lambda > 30$ the coefficient Q_{scatt} is approximated by the value 2 as indicated in figure 4a.

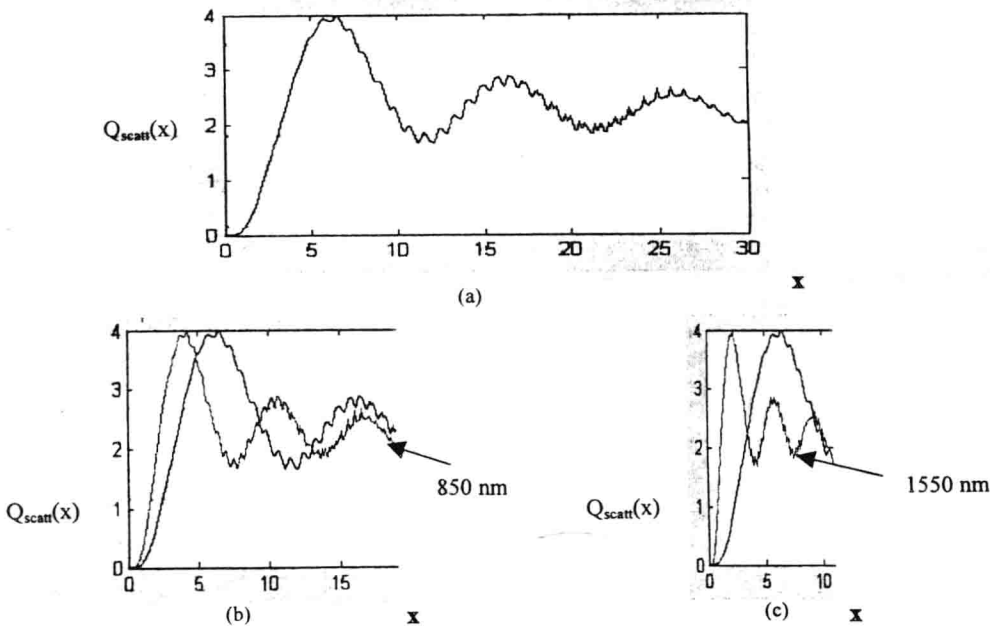


Figure 4: (a) Scattering efficiency coefficient versus the size parameter x for 550 nm wavelength. (b) Comparison between 550 nm and 850 nm. (c) Comparison between 550 nm and 1550 nm.

Given the visibility measurement V in equation (6), the corresponding attenuation at 550 nm can be derived. The highly non-linear dependency of the scattering coefficient in wavelength makes it difficult to derive the attenuation for other wavelengths. In figure (4b) and (4c) we illustrate how the scattering coefficient $Q_{\text{scat}}(x)$ varies from the visible wavelength 550 nm to 850 nm and 1550 nm.

In some references studying atmospheric attenuation of optical signals, for example [6], the following equation (9) is utilized to base the attenuation on the visibility (equation (6)) and the incident wavelength λ .

$$\beta_{\text{Scat}}(\lambda) = \beta_{\text{Scat}}(\lambda = 0.55\mu)\left(\frac{\lambda}{0.55}\right)^{-\delta} = \frac{3.91}{V}\left(\frac{\lambda}{0.55}\right)^{-\delta} \quad (\text{Km}^{-1}) \quad (9)$$

Where, the exponent $\delta = 1.6$ for good visibility, 1.3 for $V=6-50$ Km and $0.585 V^{-1/3}$ for visibility less than 6 Km. The problem with equation (9) is that the exponent value and the one-to-one relation between visibility and attenuation coefficient is independent of droplet sizes and their distributions contradicting equation (8). To further illustrate this point, let us build a hypothetical distribution model using equation (8) (figure (5a)) and that fits equation (9) for 785 nm wavelength. Of course, such a distribution does not correspond to any real life distributions in light of section two results. Now, using the same distribution (figure (5a)), the corresponding attenuations derived from equation (8) are depicted by (+) lines in figure (5b) for 1550 nm and 10 μ wavelengths respectively. The solid lines, on the other hand, correspond to the attenuations derived from equation (9). The inconsistency between equations (8) and (9) is evident especially for low visibilities where nuclei condensation and other effects occur as explained in section two.

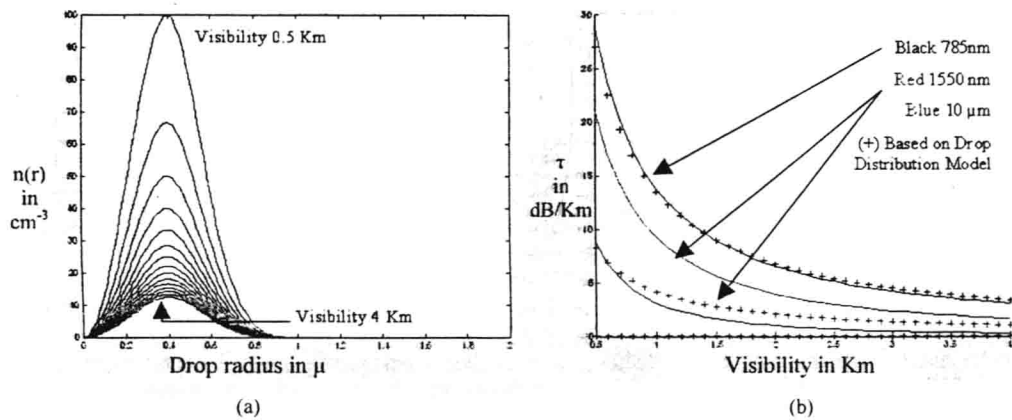


Figure 5: (a) Hypothetical fog distribution model. (b) Attenuation versus visibility. Solid lines correspond to equation (9) and (+) lines corresponds to equation (8) using the distribution in (a).

In table 3 we display some of Simulight™ results in evolving, stable and selective fogs (see table 2) and compare them to those of references [21,22] and equation (9). We adopted Arnulf's [3] fog terminology while using Simulight™ enhanced modeling technique. From table 3, it is obvious that equation (9) fails to estimate proper attenuations for visibilities below 3 Km. These three fog models were developed based on some of references [5,10,22] results as well as other published field data from different seasons and geographical locations. It is worth noting Simulight™ lower attenuation predictions for 10 μ . This result was expected since Simulight™ attenuations due to absorption are solely due to water vapor presence. For long wavelength, it is necessary to use the original Mie scattering equation with the complex value of atmospheric index of refraction which varies with temperature, pressure and wavelength [24]. A sample of Simulight™ results is provided in Table 4 in the printed report caption.

Table 2: Simulight™ weather condition definitions.

Clear Weather:	Includes light Haze and Rain: Visibilities over 4 Km.
Rainy Weather:	Weather conditions that account for rain only.
Evolving Fog:	Weather conditions between light haze, dense haze and stable fog: Visibilities between 1 and 4 Km.
Stable Fog:	Stable foggy weather conditions: Visibilities up to 1.5 Km. The low visibilities include stable low clouds.
Selective Fog:	Selective fog is more transient than stable fog with Visibilities up to 0.75 Km. This includes low clouds of short durations.

Table 3: Simulight™ results comparison in a few fog conditions.

	Fog Model	Visibility (Km)	Wavelength (nm) Simulight / Experiments	Simulight™ Mie Loss (dB/Km)	Experiment* (dB/Km)	Experiment* Day/Time	Equation (1) (dB/Km)
1a	Evolving	1	750 / 655	17.09	15.2	Dec 11, 2220	14.16
1b			1230 / 1230	18.8	17.37		10.6
1c			10,100 / 10,100	0.93	7.3		3.1
2a	Stable	0.075	750 / 655	227.06	226.2	Jan29/30 2106-2306	209.73
2b			1230 / 1230	239.2	247.33		185.64
2c			10,100 / 10,100	213.65	263.4		110.42
3a		0.30	750 / 655	57.72	62.9	Jan24 1812-1824	50.13
3b			1230 / 1230	65.78	68.4		41.3
3c			10,100 / 10,100	12.67	18.45		18.1

(*) Clay, M. R. and Leinberg, A. P., *Transmission of electromagnetic radiation in fogs in the 0.53-10.1 μ m wavelength range*, Applied Optics, Vol. 20, No. 22, 1981, page 3831

Table 4: Sample of Simulight™ report for case 3c in table III

Simulight(TM) version 4.0 -- Simulation Report	
Deployment Parameters:	
Range	= 1.000 Km
Wavelength	= 10100.000 nm
Bandwidth	= 100.000 Mbps
Weather Parameters:	
Weather Condition	= Foggy -- stable
Visibility	= 0.300 Km
Relative Humidity	= 75.000 %
Temperature	= 30.000 degree Celsius
System Parameters:	
Tx Diameter	= 5.000 cm
Number of Transmitters	= 1
Rx Diameter	= 12.000 cm
Number of Receivers	= 1
Beam Divergence	= 2.000 mrad

Tx Power	=	10.000 mW
Tx Preamplification	=	0.000 dB
Receiver Sensitivity	=	-45.000 dBm
Rx postamplification	=	0.000 dB
Other Losses	=	5.000 dB
Simulation Result:		
Calculated Visibility	=	0.310 Km
Beam Spot	=	205.000 cm
Dispersion Loss	=	-24.651 dB
Absorption Loss	=	-4.287 dB
Rainfall Loss	=	0.000 dB
Rayleigh Scattering Loss	=	-0.354 dB
Mie Scattering Loss	=	-12.678 dB
Received Power	=	-36.971 dBm
Available Link Margin	=	8.030 dBm

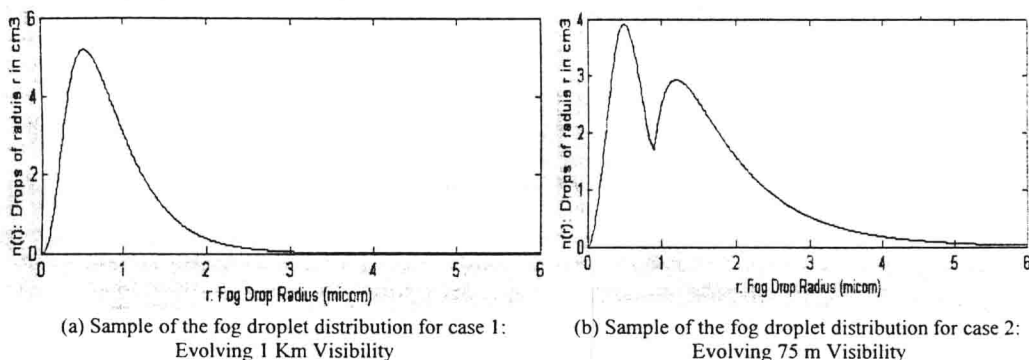


Figure 6: Samples of fog-droplet distribution models embedded in Simulight™ version 4.

Of course the key in all above computations and comparisons is Aerosol droplet size distributions. The mechanism that lies behind the analytical process to derive these distributions is UlmTech, Inc. Simulight™ proprietary. In section two we give the overall description of the process from the Atmospheric Physics point of view. In figure 6, we plot a couple of distributions utilized by Simulight™ for table 3 computations. It is clear that in some cases, bimodal distributions are necessary to reflect the physical and chemical aspects of fog and cloud formation as indicated in section two. These bimodal distributions are more apparent when the atmospheric system in equilibrium goes through low supersaturation stages. We remind the reader that supersaturation occurs when water vapor exists at higher vapor pressure than it is consistent with saturation [Goody and Walk]. For this to happen no liquid water may be present and the air is said to be supersaturated. If there are any liquid water molecules, then water vapor molecules will immediately get attached to themselves forming liquid/air surfaces. In section two we review such a mechanism in detail.

5. Conclusion

In this paper we reviewed some of the basics of thermodynamics and mechanics of fog and low clouds formation. We conclude that the Kruse equation does not hold for severe visibilities and that for a given visibility it is impossible to predict FSO attenuations since it corresponds to many different droplet size distributions. For very short-range visibilities, an estimation of the water droplet sizes and concentration is required to derive attenuation from the original Mie scattering equation. Based on our studies bimodal distributions with two radius peaks, instead of one, are used to model dense fog and cloud when large drops condensate through supersaturation, whereas smaller particles does not condensate. The fundamentals behind Simulight™, first commercial FSO weather simulator, are revisited without revealing the core technology behind distribution derivation. We compare some of Simulight™ results against published experimental results and found agreement with some fog cases. Recently, FSO vendors have adopted the backup link path to avoid answering the FSO availability question. The most popular wireless